Photoion Photoelectron Coincidence Spectroscopy of Primary Amines RCH_2NH_2 (R = H, CH_3, C_2H_5, C_3H_7, *i*-C_3H_7): Alkylamine and Alkyl Radical Heats of Formation by Isodesmic Reaction Networks

Andras Bodi,[†] James P. Kercher,[‡] Curtis Bond,[‡] Patcharica Meteesatien,[‡] Bálint Sztáray,[†] and Tomas Baer[‡,*]

Physical Organometallic Chemistry Laboratory, Institute of Chemistry, Eötvös University, Budapest, Hungary, and Department of Chemistry, University of North Carolina, Chapel Hill, North Carolina 27599-3290

Received: July 25, 2006; In Final Form: October 2, 2006

Alkylamines (RCH_2NH_2, R = H, CH_3, C_2H_5, C_3H_7, *i*-C_3H_7) have been investigated by dissociative photoionization by threshold photoelectron photoion coincidence spectroscopy (TPEPICO). The 0 K dissociation limits (9.754 ± 0.008, 9.721 ± 0.008, 9.702 ± 0.012, and 9.668 ± 0.012 eV for R = CH_3, C_2H_5, C_3H_7, *i*-C_3H_7, respectively) have been determined by preparing energy-selected ions and collecting the fractional abundances of parent and daughter ions. All alkylamine cations produce the methylenimmonium ion, $CH_2NH_2^+$, and the corresponding alkyl free radical. Two isodesmic reaction networks have also been constructed. The first one consists of the alkylamine parent molecules, and the other of the alkyl radical photofragments. Reaction heats within the isodesmic networks have been calculated at the CBS-APNO and W1U levels of theory. The two networks are connected by the TPEPICO dissociation energies. The heats of formation of the amines and the alkyl free radicals are then obtained by a modified least-squares fit to minimize the discrepancy between the TPEPICO and the *ab initio* values. The analysis of the fit reveals that the previous experimental heats of formation are largely accurate, but certain revisions are suggested. Thus, $\Delta_f H^o_{298K}$ [CH_3NH_2(g)] = −21.8 ± 1.5 kJ mol^{-1}, $\Delta_f H^o_{298K}$[$C_2H_5NH_2$(g)] = −50.1 ± 1.5 kJ mol^{-1}, $\Delta_f H^o_{298K}$[$C_3H_7NH_2$(g)] = −70.8 ± 1.5 kJ mol^{-1}, $\Delta_f H^o_{298K}$[$C_3H_7^\bullet$] = 101.3 ± 1 kJ mol^{-1}, and $\Delta_f H^o_{298K}$[*i*-$C_3H_7^\bullet$] = 88.5 ± 1 kJ mol^{-1}. The TPEPICO and the *ab initio* results for butylamine do not agree within 1 kJ mol^{-1}; therefore, no new heat of formation is proposed for butylamine. It is nevertheless indicated that the previous experimental heats of formation of methylamine, propylamine, butylamine, and isobutylamine may have been systematically underestimated. On the other hand, the error in the ethyl radical heat of formation is found to be overestimated and can be decreased to ± 1 kJ mol^{-1}; thus, $\Delta_f H^o_{298K}$[$C_2H_5^\bullet$] = 120.7 ± 1 kJ mol^{-1}. On the basis of the data analysis, the heat of formation of the methylenimmonium ion is confirmed to be $\Delta_f H^o_{298K}$[$CH_2NH_2^+$] = 750.3 ± 1 kJ mol^{-1}.

Introduction

Primary alkylamine ions have a peculiar property in that they dissociatively ionize with the production of the methylenimmonium ion, $CH_2NH_2^+$. Thus, the reaction:

$$RCH_2NH_2 + h\nu \rightarrow CH_2NH_2^+ + R^\bullet + e^- \qquad (1)$$

where $R^\bullet$ = $H^\bullet$, $CH_3^\bullet$, $C_2H_5^\bullet$, $C_3H_7^\bullet$, and *i*-$C_3H_7^\bullet$, is driven by the considerable stability of the methylenimmonium cation and results in the production of a variety of alkyl free radicals. An accurate determination of this dissociative photoionization onset can lead to accurate heats of formation of the alkylamines or the free radicals. Since this reaction involves a simple bond break in the alkylamine cation, we do not expect there to be a reverse barrier. Indeed, our modeling of the butylamine case indicates that the transition state is very loose.

Harvey and Traeger reported dissociative photoionization onsets for these amines using photoionization mass spectrometry (PI-MS) in which the fragment ion signal is recorded as a function of the photon energy.[1] The strategy in their study was to assume that both the amine and the free radical heats of formation are well established. An average value for the heat of formation of the methylenimmonium ion was thus derived.

The purpose of the present study is to use the technique of threshold photoelectron photoion coincidence (TPEPICO) spectroscopy to obtain more reliable dissociation energies than is possible with photoionization mass spectrometry. Two isodesmic reaction networks are then built, and the calculated reaction heats are related by means of the experimental onset energies. Thus, self-consistent heats of formation can be obtained for both the alkylamines and the alkyl free radicals. The latter values have fluctuated over the years and they have only recently been obtained with any degree of reliability as a result of neutral kinetic studies in which the forward and backward rate constants of such reactions as:

$$R^\bullet + HBr \leftrightarrow Br^\bullet + RH \qquad (2)$$

have been studied. In particular, Seakins et al.[2] measured the temperature-dependent rate constants for the forward and reverse reactions of eq 2 with various alkyl groups, including $C_2H_5^\bullet$, *i*-$C_3H_7^\bullet$, *s*-$C_4H_9^\bullet$, and *t*-$C_4H_9^\bullet$. The equilibrium constant from

* Author to whom correspondence should be addressed. E-mail: baer@unc.edu.
[†] Eötvös University.
[‡] University of North Carolina, Chapel Hill.

10.1021/jp064739s CCC: $33.50
Published on Web 11/22/2006

the ratio of the forward and the backward rate constants measured as a function of the temperature then leads to both a $\Delta_r H°$ and $\Delta_r S°$. Past history has shown that measurements by a single technique are not reliable until corroborated by other methods,[3] in part because all measurements rely on ancillary thermochemical information. The ion cycle such as used by Harvey and Traeger and by us is among the most reliable approaches for determining accurate thermochemistry, and the results are often obtained with a precision of ± 1 kJ mol^{-1}. Furthermore, as they depend upon completely different ancillary heats of formation than the neutral studies, they provide an independent verification of the latter values.

A common ion cycle used to obtain free radical heats of formation involves measuring the energies of even electron ions, e.g., CH_3^+, which can be obtained accurately from the dissociative photoionization of methane or methyl halides. This ion heat of formation can be combined with the free radical ionization energy to obtain the free radical heat of formation. However, because of the severe geometry change of the alkyl radicals upon ionization (other than the methyl radical), it is very difficult to extract the adiabatic ionization energy from such photoionization or photoelectron spectroscopic studies.[4−7] Thus, the reaction outlined in eq 1 represents a welcome avenue for examining alkyl radical heats of formation through a different ion cycle.

The major advantage of TPEPICO over the PI-MS method is that in the former, the ions are energy selected so that the fractional abundance of the fragment and parent ions can be obtained as a function of the ion internal energy, the so-called breakdown diagram. The breakdown diagram is independent of changing photoabsorption cross-sections, i.e., Franck−Condon factors for producing ions at certain energies. As a result, its shape is determined solely by the neutral molecule's thermal energy distribution and the dissociation onset when the photodissociation is fast. Since the molecule's thermal energy distribution can be easily modeled, the 0 K dissociation onset is readily established. Of equal importance is the effect of slow rate constants. The fragment ion signal in PI-MS contains few clues about the dissociation rates. If these are so slow that the parent ions cannot dissociate in the time scale of the experiment, typically within tens of microseconds, the observed onset is shifted to higher energies by the kinetic shift.[8−10] In PI-MS studies, slow onsets can only be divined from RRKM calculations that depend on assumed transition state properties. By contrast, the TPEPICO ion time-of-flight (TOF) distributions show clear asymmetry when the reactions are slow, and the TOF profiles can be modeled with directly measured rate constants.

Experimental Details

The apparatus has been described in detail elsewhere,[11] so only a brief overview is presented here. Ions are generated by photoionization with vacuum UV light from a hydrogen discharge lamp. The quasicontinuous light is dispersed by a 1 m normal incidence monochromator with 100 μm slits to give a resolution of 1 Å, which translates to 7 meV (0.7 kJ mol^{-1}) at the onset energies obtained in this study (approximately 9.7 eV). Electrons and ions are accelerated out of the ionization region in a field of 20 V cm^{-1}. Threshold electrons are selected by velocity focusing electrons with zero perpendicular momentum to the extraction axis onto a 1.5 mm aperture located 12 cm from the ionization region. Since energetic electrons with initial velocity vectors directed parallel with the extraction axis are also focused onto this aperture, the threshold electron signal is contaminated with "hot" electrons. This hot electron contamination is accounted for by collecting a second set of electrons, whose trajectory ends in a 2 mm $\times$ 5 mm rectangular aperture close to the central aperture. Channeltron electron multipliers located behind these apertures collect the central and the off-axis signals. Since the electrons collected by the off-axis rectangular aperture are a good representation of the hot electrons at the central collector, we can subtract a constant fraction of the off axis signal from the central signal and thus obtain a pure threshold electron signal, as described in previous publications.[12−14]

Each of the two electron signals are sent to time-to-pulse-height converters (TPHC) and are used as start signals for the ion time-of-flight (TOF) measurement. The ion signals provide the stop signals for both TPHC's. The outputs from the two units are then sent to two multichannel pulse height analyzers which display the ion TOF distributions for both the central and the off-axis electron signals. Experiments were carried out at various photon energies in the vicinity of the dissociation onsets. Typical TOF distributions required between 1 and 2 h to collect. A reflectron was used to carry out the TOF-analysis of the ions, but part of the data acquisition was repeated in a two-stage linear TOF,[15] which is better optimized for the study of metastable ion dissociations in which the mass of the leaving fragment is commensurable with that of the product ion.[8] The collection efficiency, η, for the zero energy electrons and the ions were obtained at the threshold photoionization limit for acetylene (11.4 eV) from the usual relation: $\eta(e^-) = C/I$, where C and I are the coincidence and total ion counts per second, respectively, and $\eta(M^+) = C/E$, where E is the electron counts per second. Typical efficiencies were 40% for electrons, 12% for ions through the reflectron mass spectrometer, and twice this if the linear TOF tube was employed. The photon energy was calibrated using the intense Lyman-α emission line of the light source at 1215.65 Å.

The experimental results consist of the ion TOF distributions at various photon energies. The fractional abundances of the various parent and fragment ions were corrected for the hot electron contribution and plotted as a function of the photon energy to produce the breakdown diagram. In some cases, the TOF distribution of the fragment ion exhibited an asymmetry, which is characteristic of slow dissociations. The asymmetry was modeled in order to extract the ion dissociation rate constants as a function of the ion internal energy.

Results

Although all of the reactions produce the very stable CH_2-NH_2^+ ion, hydrogen atom loss has also been observed for ethylamine. In addition, butylamine and, to a small degree, isobutylamine formed metastable ions, which dissociated slowly on the mass spectral time scale. That is, the minimum rate constant was less than 10^7 s^{-1}, which caused the daughter ion TOF distribution to be asymmetric. The observed onsets for such metastable reactions can be shifted toward higher energies so that the rate constants must be taken into account in the modeling.

The RRKM modeling procedure was used as described in earlier publications.[9,16] The required neutral, ion, and transition state frequencies and rotational constants were calculated at the B3LYP/6-311+G(d,p) level. The transition state geometry was obtained by constrained optimization: the bond length between the leaving alkyl radical fragment and the nitrogen atom was fixed at 4 Å. The frequencies and rotational constants were used to calculate the density of states of the ions and the number of

states of the transition states. Since only the butylamine photodissociation proved to be slow, the actual values of the densities and numbers of states are only important in the butylamine modeling, in which the TS frequencies have been fit to reproduce the measured rate information and account for the kinetic shift. The ionization energy is almost irrelevant in the modeling of fast reactions but becomes an important parameter if the photodissociation is slow, because the ion density of states depends on the ion internal energy, which is a function of the ionization energy as well. As auxiliary results, the ionization energies are also discussed for each species, but they only influence the dissociation energy determination for the butylamine, for which the calculated and the previously reported ionization energies agree well.

Methylamine. As the methylamine TPEPICO experiment has been published elsewhere,[17] we only quote the results here. The methylamine ion loses an H atom by tunneling through a small barrier of approximately 2 kJ mol^{-1} to generate the methylenimmonium ion, $CH_2NH_2^+$ in the 10.00 eV < $h\nu$ < 10.30 eV energy range. Although the reaction is slow ($k < 10^7$ s^{-1}, close to the onset), it is sufficiently fast that the appearance energy is not shifted to higher energy by the kinetic shift. Thus, the experimental breakdown diagram agrees well with the RRKM model, and the absence of a kinetic shift makes the onset straightforward to determine. The experimental 10.228 ± 0.008 eV 0 K dissociation energy is 18 meV higher than the 10.21 eV reported by Harvey and Traeger.[1] On the other hand, it agrees very well with the 10.226 eV dissociation energy calculated[17] with the W1U method as implemented in Gaussian 03[18] and serves as a reliable basis to calculate the methylenimmonium 0 K heat of formation, which can then be employed as a starting point in the isodesmic reaction network fit. The 0 K TPEPICO onsets can be converted to room-temperature reaction heats by the equation:

$$\Delta_r H^\circ_{298K} = \Delta_r H^\circ_{0K} + \Sigma(H^\circ_{298K} - H^\circ_{0K})_{products} - \Sigma(H^\circ_{298K} - H^\circ_{0K})_{reactants} \quad (3)$$

where $H^o_{298K} - H^o_{0K}$ are known for the elements, certain radicals and molecules,[19,20] but need to be calculated for small molecules. The 10.228 eV 0 K dissociation energy converts to 10.278 eV, or $\Delta_r H^o_{298K} = 991.7$ kJ mol^{-1}, which is the 298 K photodissociation enthalpy.

Ethylamine. The breakdown diagram for the ethylamine ion is shown in Figure 1. Although the dominant reaction generates the $CH_2NH_2^+ + CH_3^\bullet$ products, a small amount of hydrogen atom loss product (less than 10%) was also observed, in agreement with the findings of Harvey and Traeger.[1] By analogy with the H loss reaction in methylamine, and the fact that this channel disappears completely at 9.75 eV, we conclude that the H loss reaction is slow, probably a result of tunneling. Thus, when the ion energy lies below that of the $CH_2NH_2^+$ channel, the ion has no choice but to dissociate via H loss. But once the ion energy lies in excess of the $CH_2NH_2^+$ onset, the H loss channel cannot compete and becomes insignificant. The CBS-APNO[21]-calculated onset for H-loss of 9.627 eV lies 135 meV below the similarly computed onset of the methyl loss (9.762 eV), which corroborates this assumption. We thus added the parent and H loss signals together, which are shown as solid parent ion points in the breakdown diagram. The calculated solid lines are determined solely by the molecule's thermal energy distribution, which includes three external rotational degrees of freedom, and the 0 K dissociation limit, the latter being the only adjustable parameter in the fit.

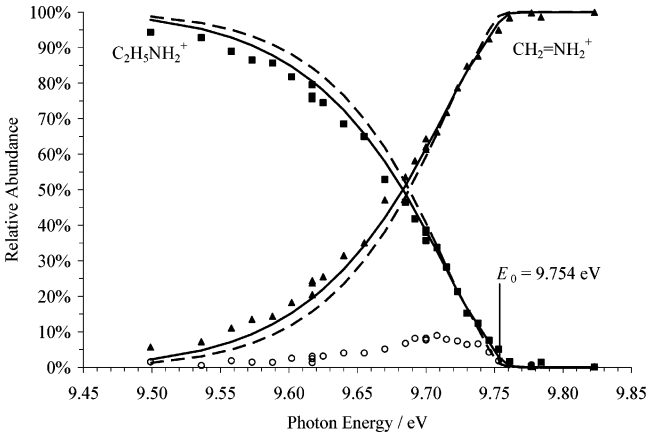

Figure 1. Ethylamine breakdown diagram. Dots correspond to the experimental data, the continuous (320 K) and dashed (298 K sample temperature) lines are from the RRKM modeling of the experiment. The empty circles correspond to H atom loss, which is a slow process that cannot compete with the CH_3 loss. Thus, it is added to the parent ion partial abundance in the modeling (see text).

Two simulations are shown in Figure 1, one for a 298 K and the other for a 320 K thermal sample. Even though the latter gives a much better fit, especially at low photon energies that correspond to high thermal energies, the derived 0 K onsets (9.749 and 9.754 eV) agree quite well. This is because the extraction of the dissociation energy for fast reactions depends mainly on the low-energy part of the thermal energy distribution where the two temperature fits are very similar. Still, the reason for the better fit with a 320 K sample temperature is of some interest. By raising the temperature, we broaden the thermal energy distribution, which increases the high-energy tail of the distribution thus providing a better fit at low photon energies. For fast dissociations, the sum of the photon and the thermal energies has to exceed the dissociation onset in order for the dissociation to occur, i.e., $h\nu + E_{th} > E_0$. The calculated thermal energy distribution depends on the assumed vibrational frequencies. It is thus possible that our calculated frequencies are too high. We found that in order to obtain a 298 K fit equivalent to 320 K fit, it was necessary to reduce the four lowest frequencies of the ethylamine molecule from 238, 270, 414, and 797 cm^{-1} to 100 cm^{-1}, each. This is clearly an unreasonable adjustment of the frequencies. On the other hand, if ethylamine molecules with high thermal energy have a larger photoionization cross-section, they may be slightly overrepresented in the ion manifold, which may also account for the higher than expected low photon energy tail in the breakdown diagram.

The E_0 of 9.754 ± 0.008 eV is 37 meV higher than the 0 K onset reported by Harvey and Traeger[1] but is only 12 meV lower than the computed W1U onset of 9.766 eV. The excellent agreement between the W1U onset and the experimental one confirms the accuracy of the onset determination. The discrepancy of our onset with that of Harvey and Traeger is comparable to previous results on other molecules such as C_3H_7I[22,23] and acetone.[24,25] The 0 K dissociation energy of ethylamine can be converted to $\Delta_r H^o_{298K} = 947.4$ kJ mol^{-1} photodissociation enthalpy.

The ionization energy of ethylamine is reported to be in the 8.8 − 8.9 eV range in the NIST compilation.[26] This is in good agreement with the calculated values: 8.885, 8.883, and 8.883 eV at the W1U, CBS-APNO, and G3B3 levels of theory, respectively.

Propylamine. The photodissociation of propylamine is characterized by only a single product ion, $CH_2NH_2^+$, up to at

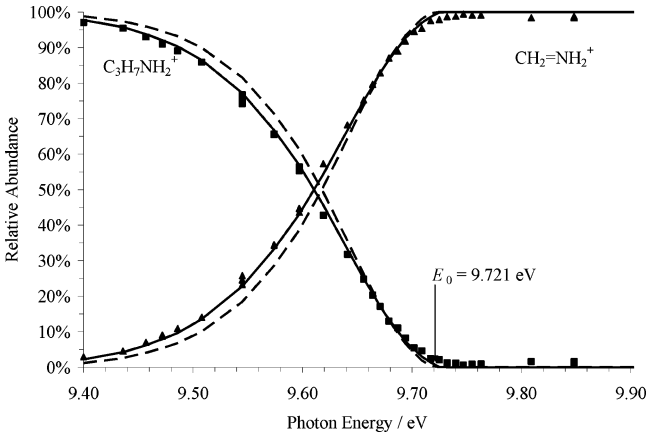

Figure 2. Propylamine breakdown diagram. Dots show the experimental data, solid lines correspond to the 320 K, dashed lines to the 298 K RRKM model of the experiment.

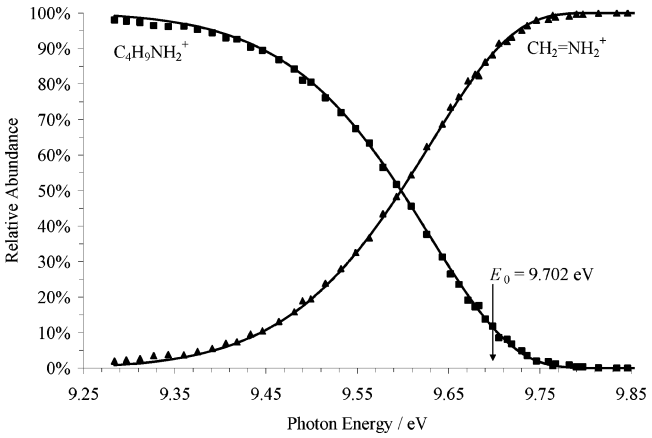

Figure 3. Butylamine breakdown diagram. Dots show the experimental data, solid lines correspond to the RRKM model of the experiment.

least 10 eV. The breakdown diagram in the vicinity of the dissociation limit is shown in Figure 2. As in the case of ethylamine, the calculated breakdown diagram fits the experimental one very well if the temperature is raised to 320 K, and as before, the derived onset optimized to fit the data near the 0 K onset is quite invariant to the assumed temperature. The derived onset energy of 9.721 ± 0.008 eV is 53 meV higher than that reported by Harvey and Traeger but only 4 meV lower than the W1U value. It can be converted to a photodissociation enthalpy of $\Delta_r H^o_{298K}$ = 941.8 kJ mol^{-1}.

The propylamine ionization energy was calculated to be 8.788, 8.749, and 8.780 eV at the W1U, CBS-APNO, and G3B3 levels of theory, respectively. This is in contrast with the 8.5 eV reported by Aue, Webb, and Bowers[27] but in good agreement with the photoionization mass spectroscopy result of 8.78 ± 0.02 eV of Watanabe and Mottl.[28] On the basis of the above calculations, we suggest that the propylamine ionization energy is closer to the Watanabe value, i.e., 8.77 ± 0.02 eV.

***n*-Butylamine and *i*-Butylamine.** The *n*-butylamine breakdown diagram, shown in Figure 3, is considerably broader than those of the smaller amines because of the broader thermal energy distribution. In addition, the TOF distributions showed a slight asymmetry near the dissociation onset, which indicates that the reaction is slow. We used the linear time-of-flight tube instead of the reflectron to obtain the breakdown diagram, so that the rate constants could also be extracted from the TOF distributions. The rate constants are then used in the RRKM

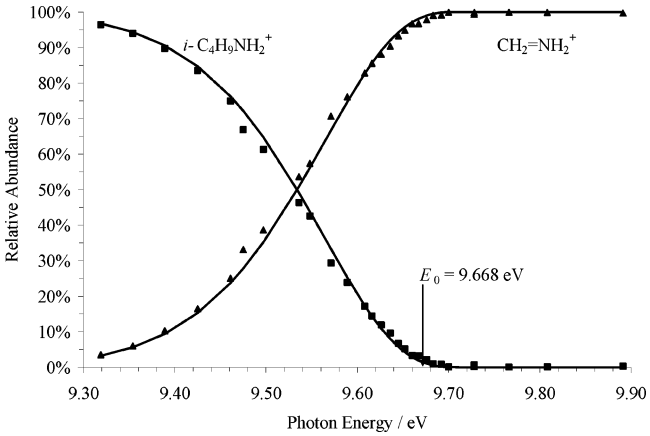

Figure 4. Isobutylamine breakdown diagram.

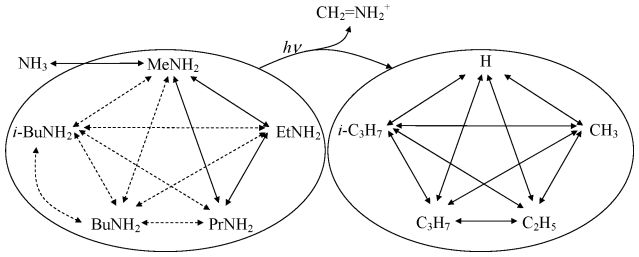

Figure 5. Isodesmic reaction networks. Continuous arrows designate W1U calculations, dashed arrows CBS-APNO isodesmic reaction heats, and the direct isomerization of *i*-butyl/*n*-butylamine. The connection between the two networks is constituted by the TPEPICO dissociation energies.

modeling to extrapolate to the 0 K dissociation energy and assess the kinetic shift, which was estimated to be 5.4 kJ mol^{-1}. The 0 K dissociation energy of the *n*-butylamine ion was found to be 9.702 ± 0.012 eV. The *i*-butylamine TOF distributions hardly showed an asymmetry, and the kinetic shift was estimated to be less than 1 kJ mol^{-1}. The breakdown curve for *i*-butylamine and the 0 K dissociation energy (9.668 ± 0.012 eV) are shown in Figure 4. The 298 K photodissociation enthalpies are, thus, $\Delta_r H^o_{298K}[BuNH_2 - Pr\bullet]$ = 939.9 kJ mol^{-1} and $\Delta_r H_{298K}{}^o[i\text{-}BuNH_2 - i\text{-}Pr\bullet]$ = 935.9 kJ mol^{-1}.

The CBS-APNO and G3B3 calculated ionization energy for butylamine (8.679, and 8.710 eV, respectively) agree well with the 8.7 eV reported by Aue and Bowers.[29] The CBS-APNO and G3B3 calculated isobutylamine ionization energies (8.632, and 8.684 eV, respectively) are slightly outside the error bar of the reported 8.5 ± 0.1 eV.[27]

***Ab Initio* Calculations.** Although the alkylamine molecules appear to have well established heats of formation,[30] we checked these numbers with a series of *ab initio* calculations. These were carried out at the ITS Research Computing facility of the University of North Carolina using G3B3,[31] CBS-APNO,[21] and W1U[32,33] levels of theory with the Gaussian03 program suite.[18] The results were used to confirm the measured onsets and to create two networks of isodesmic reactions as presented in Figure 5. There is one amine network, consisting of the primary amines, and one alkyl radical network made up by the corresponding photofragmentation products. The link between the two is provided by the TPEPICO experiment, the onsets equaling the 0 K reaction heats of the photodissociation steps, reaction 1. The 298 K heats of formation of the species were subsequently optimized to achieve self-consistency.

TABLE 1: Literature 298 K Heats of Formation and Their Conversion to 0 K[a]

	$\Delta_f H°_{298K}$ (lit)	$H_{298K} - H_{0K}$ (kJ mol^{-1})	$\Delta H_{rot}{}^{\dagger}$	$\Delta_f H°_{0K}$
NH_3	-45.9 ± 0.4	10.0	−	−38.9
CH_3NH_2	-23.4 ± 1	11.7	0.17	−8.4
$C_2H_5NH_2$	-47.5 ± 0.6	14.6	0.36	−25.7
$C_3H_7NH_2$	-72.1 ± 0.4	18.1	0.53	−44.6
$C_4H_9NH_2$	-91.8 ± 1.1	21.5	0.67	−58.4
i-$C_4H_9NH_2$	-98.6 ± 0.5	22.3	0.68	−65.8
H•	218.0[c] $\pm$ 0.01	6.2	−	216.0
CH_3•	146.7[d] $\pm$ 0.3	10.5	−	149.9
C_2H_5•	120.9[e] $\pm$ 1.7	11.7	−1.30	132.5
C_3H_7•	100.8[f] $\pm$ 2.1	15.0	−0.60	118.6
i-C_3H_7•	90.0[g] $\pm$ 1.7	15.1	−1.10	107.7
H_2O	-241.8 ± 0.04	9.9	−	−238.9
CH_3OH	-201.5 ± 0.2	11.2	−0.10	−190.3
C_2H_5OH	-235.2 ± 0.3	14.1	0.18	−217.5
C_3H_7OH	-255.1 ± 0.4	17.4	0.33	−231.1
C_4H_9OH	-274.9 ± 0.4	20.9	0.57	−244.9
i-C_4H_9OH	-283.8 ± 0.8	20.7	0.45	−253.7
CH_4	-74.4 ± 0.4	10.0	−	−66.4
C_2H_6	-83.8 ± 0.3	11.9	0.16	−68.2
C_3H_8	-104.7 ± 0.5	14.9	0.37	−82.6
C_4H_{10}	-125.7 ± 0.6	18.4	0.51	−97.5
C_5H_{12}	-146.9 ± 0.8	21.8	0.65	−112.7
i-C_5H_{12}	-153.6 ± 0.9	21.6	0.58	−119.1
$NH_2CH_2^+$	750.4[f] $\pm$ 1.3	10.4	−	762.2

[a] Unreferenced $\Delta_f H°_{298K}$ (lit) data are from the Pedley compilation.[30] [b] The correction of internal rotation to the thermal energy calculated according to eq 5. This is the 298 K energy difference between treating these modes as low-frequency vibrations and hindered rotors. $H_{298K} - H_{0K}$ data are calculated at the B3LYP/cc-pVTZ+d level for species with less than five heavy atoms, at B3LYP/6-311+G(d,p) level for others, and include corrections for internal rotation. W1U and CBS-APNO calculations refer to 0 K energies with zero-point vibrational energy. [c] Wagman et al.[20] [d] Ruscic et al.[44] [e] Sander et al.[45] [f] Atkinson et al.[49] [g] Seakins et al.[2] [h] Bodi et al.[17]

The isodesmic reaction networks consist of the following reactions:

$$RNH_2 + R'OH \rightarrow ROH + R'NH_2 \quad (4a)$$

$$RNH_2 + R'CH_3 \rightarrow RCH_3 + R'NH_2 \quad (4b)$$

$$R^{\bullet} + R'H \rightarrow RH + R'^{\bullet} \quad (4c)$$

where R• and R′• correspond to different alkyl chains. The solid lines within the networks in Figure 5 denote isodesmic reaction heats calculated with W1U theory, and the dashed lines refer to those calculated with the CBS-APNO theory. Isobutylamine and butylamine may isomerize isodesmically, which was also included in the network at the CBS-APNO level (bent arrow). The alkane and alkyl alcohol heats of formation were taken from the literature[30] and were assumed to be accurate (see thermochemical data in Table 1). A total of 45 reactions, available as Supporting Information, were calculated at the two levels of theory.

Internal Rotation. The conversion (eq 3) of 0 K heats of formation to 298 K data often relies on *ab initio* thermal enthalpies, which are typically calculated based on the harmonic oscillator approximation to internal molecular motions. The effect of internal rotation on the thermal energy is thus important to consider when determining accurate 298 K heats of formation. Figure 6 shows an ethylamine potential energy surface, which was acquired by constrained optimizations at the B3LYP/6-311+G(d,p) level. The surface shows that the two internal rotational modes are almost perpendicular, and the barriers to internal rotation are 13.6 kJ mol^{-1} for the methyl group and 9.4 kJ mol^{-1} for the amine group. To estimate the internal rotational correction to the thermal enthalpy, we used the two lowest harmonic vibrational frequencies of 270 cm^{-1} and 238 cm^{-1}, handled the two internal rotational coordinates as independent, and employed eq 5, first derived by McClurg et al.[34] and corrected by Knyazev:[35]

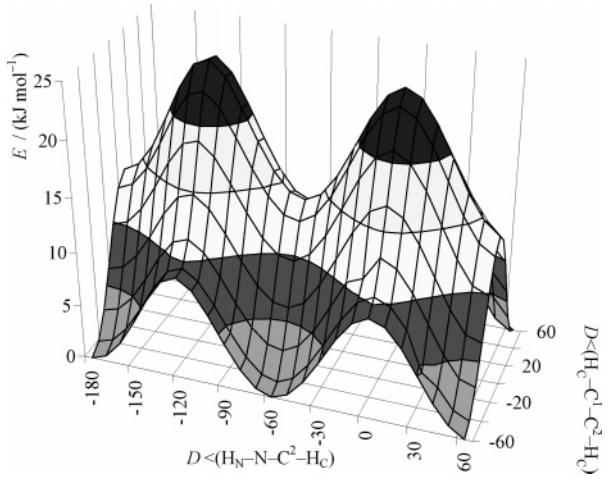

Figure 6. Ethylamine internal rotational potential energy surface. The two internal rotational motions appear to be perpendicular with respect to each other.

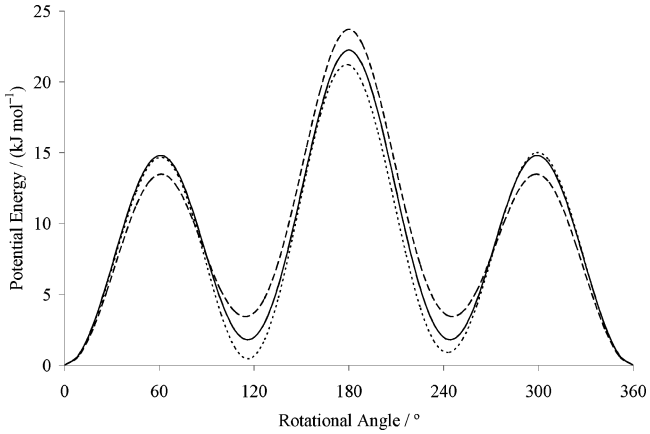

Figure 7. Propylamine (solid line), propanol (dotted line) and butane (dashed line) internal rotational potential energy curves around the center carbons as the axis. Similar energy curves result in similar internal rotational corrections, i.e., the internal rotational corrections will mostly cancel out in the isodesmic reaction networks.

$$\Delta H/kT = -\frac{1}{2} - \frac{1}{(2+16r)\Theta} + \frac{r}{2\Theta}\left(1 - \frac{I_1[r/2\Theta]}{I_0[r/2\Theta]}\right) \quad (5)$$

where r is the ratio of the internal rotation barrier height and the harmonic oscillator frequency, $V_0/\hbar\omega$, and $\Theta = \hbar\omega/kT$, *i.e.* a nondimensional temperature, and I_1 and I_0 denote the first and 0th order modified Bessel functions of the first kind.[36] The ratio r is an approximate number of quantum levels within the internal rotational well. The internal rotational contribution to the thermal enthalpy is estimated to be only 0.36 kJ mol^{-1}, which is less than the uncertainty associated with its heats of formation.

Thermal enthalpy considerations also played a role in constructing the isodesmic reaction networks. Since amines, alcohols, and the corresponding alkanes have similar internal rotational potential energy surfaces (Figure 7), errors in the thermal enthalpy calculations will cancel out in isodesmic

reactions. But accurate thermal energies are nevertheless important for converting 0 to 298 K heats of formation.

Internal rotational curves were calculated for all species (amines, alkanes, alcohols, and alkyl radicals) and are available as Supporting Information. Simple dihedral angles were chosen as rotational coordinates, and when the barriers along one curve were unequal, their average was used together with the frequency of the most descriptive vibration in eq 4 to estimate the internal rotational contribution. The contributions, listed in Table 1, are usually quite small, with the exception of alkyl radicals, in which the methyl rotation is often practically barrierless, and the harmonic oscillator model significantly overestimates the thermal enthalpy.

Discussion and Extraction of Thermochemical Values

The simplest approach to extract heats of formation from the thermochemical cycles associated with eq 1 is to assume the heats of formation of two of the species so that the third one is determined by the TPEPICO onset energy. However, which of the values are we to believe: the amine heats of formation, those of the free radicals, or of the $CH_2NH_2^+$? In order to answer this question we decided to introduce further information in the form of calculated enthalpies of isodesmic reactions using a series of alcohols and alkanes. This method is, of course, vulnerable to errors in the heats of formation of the auxiliary species, but the approach has been shown to be more reliable than atomization heats in estimating heats of formations.[38−40] The calculated energies are then used along with the TPEPICO energies to find the optimum enthalpies of formation of the amines, the alkyl radicals, and the $CH_2NH_2^+$ ion. In this scheme, we accept the alcohol and alkane heats of formation as inputs and use the calculated reaction heats and the measured onset energies to determine the heats of formation of the alkylamines and the alkyl radicals. The calculated reaction enthalpies with the previous experimental amine and radical heats of formation from the literature and with the newly obtained ones are available as Supporting Information. In particular, we note that the reactions between the alcohols and the alkanes themselves exhibit only small discrepancies, which underline the fact that the heats of formation of alcohols and alkanes are probably among the best known, and justifies their use as anchors for this study.

Self-Consistent Isodesmic Reaction Networks. The methylenimmonium ion serves as a common liaison between the primary amines and the corresponding alkyl radicals. The least error prone approach to interpret the experimental and computational data thus involves their simultaneous analysis, so that neither local nor global inconsistencies remain.

Our approach is reminiscent of that of Ruscic et al.,[41] who have created Active Thermochemical Tables to determine accurate heats of formation for several key compounds. However, they had recourse to a multitude of experimental data, which enabled them to home in on several heats of formation with unprecedented accuracy. Relying on a dataset acquired by a single method (i.e., TPEPICO dissociation energies or *ab initio* calculations, as in our case) means that only a moderate improvement is expected in the heat of formation error bars, and that systematic errors in the calculations will not be compensated for by results from different methods. Consequently, the use of TPEPICO onsets connecting alkylamine and alkyl radical heats of formation through the methylenimmonium ion heat of formation as well as the calculated isodesmic reaction heats is advantageous to improve the accuracy of the derived alkylamine and alkyl radical heats of formation.

In order to optimize the amine and the radical heats of formation, a measure of the error is required, which we define by the expression:

$$\epsilon_i = \frac{(\Delta_r H[\text{calc}] - \Delta_r H[\text{from } \Delta_f H])^2}{\sigma \sum_i \delta_i} \qquad (6)$$

for the isodesmic reaction i where $\Delta_r H$[calc] denotes the best *ab initio* reaction heat (W1U where all species contain no more than four heavy atoms, CBS-APNO otherwise), σ depends on the level of theory (2 for W1U and 3 for CBS-APNO), $\Delta_r H$[from $\Delta_f H$] is the heat of reaction based on the heats of formation of the reactants and the products, and δ_i denotes the sum of the reported uncertainties in the heat of formation data of the supplementary species in the reaction. The numerator is to the second power so that large deviations from the self-consistent optimum are more penalized than small, statistically insignificant errors. The errors within a network are summed, and the overall error is given by

$$\xi = \lambda \cdot \sum_i \epsilon_i(1) + \sum_j \epsilon_j(2) + \sum_k \xi_k(\text{PEPICO}) \qquad (7)$$

where $\epsilon_i(1)$, and $\epsilon_j(2)$ are the errors from the amine and the alkyl radical networks, respectively, and $\xi_k = (\Delta_r H_k[\text{PEPICO}] - \Delta_r H_k[\text{from } \Delta_f H])^2$, *i.e.* the square of the difference between the experimental TPEPICO 298 K reaction enthalpy and the reaction enthalpy based on the heats of formation for each of the primary amines. The λ coefficient is 1 when only one of the alkane and the alcohol networks are included in the first term, while 1/2 if both are included. The heat of formation and reaction heat data are always expressed in kJ mol^{-1} in eqs 6 and 7, and the resulting error function is considered as a dimensionless quantity.

The alkylamine and the alkyl radical heats of formation were then optimized in an Excel program so that the overall error was minimized using the Generalized Reduced Gradient Method.[42] Table 1 lists the literature values that were used as a starting point in the heat of formation optimization.

The *changes* to the heats of formation in five slightly different optimizations, minimizing the total error ξ, are plotted in Figure 8. The light gray bars labeled (full) designate the optimization that takes into account the experimental results as well as the calculations. In the fitting process, the error function of the amine/alcohol network decreased from 49.2 to 1.2, that of the amine/alkane network from 34.2 to 6.6, and that of the alkyl radical network from 14.8 to 0.5. This can be compared with the 5.2 error function of the alcohol/alkane cycle (for more details see Supporting Information). The new heats of formation from the (full) procedure are also summarized in Table 2. The following two optimizations in Figure 8 are similar to the first one, except that in the bar designated (ROH) only the alcohol containing isodesmic reactions in the amine network are included, and in the (RH) designated bar, only the alkane reactions are present in the amine network. This is done so that discrepancies in the heats of formation of the alcohols or alkanes might show up. The (nolink) fit is purely *ab initio* and the last part in eq 7, *i.e.* the TPEPICO error is not considered. The full optimization results are also shown without the internal rotational corrections (norot). The methyl radical heat of formation has been determined very accurately and has the same error bar as methane (0.4 kJ mol^{-1}).[43] This value has recently been confirmed by Ruscic et al.[44] and was thus considered to be

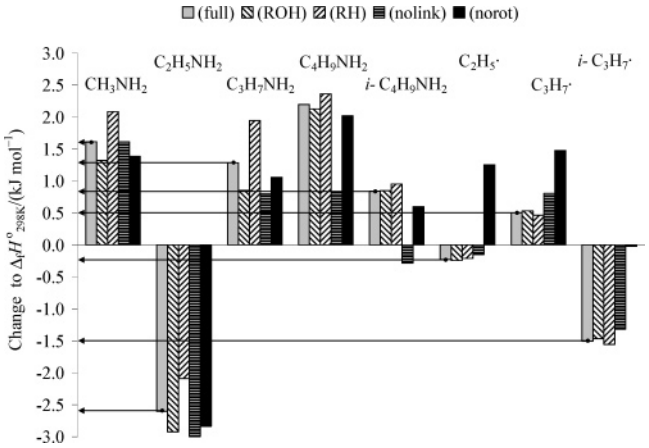

Figure 8. Optimized corrections to 298 K heats of formation based on isodesmic reaction networks connected by TPEPICO experimental dissociation energies. (full) full optimization with internal rotational corrections, (ROH) optimized without the alkane isodesmic reactions in the amine network, (RH) optimized without the alcohol isodesmic reactions, (nolink) optimization of the amine and the alkyl radical networks without the TPEPICO dissociation energies, (norot) full optimization without internal rotational corrections.

TABLE 2: New Heats of Formation Resulting from This Work

	$\Delta_f H_{298K}{}^o$/(kJ mol^{-1})	$\Delta_f H_{0K}{}^o$
CH_3NH_2	-21.8 ± 1.5	-7.0
$C_2H_5NH_2$	-50.1 ± 1.5	-28.6
$C_3H_7NH_2$	-70.8 ± 1.5	-43.3
$C_4H_9NH_2$	-89.6 ± 2.0	-56.1
i-$C_4H_9NH_2$	-97.8 ± 1.0	-64.9
C_2H_5·	120.7 ± 1.0	132.3
C_3H_7·	101.3 ± 1.0	119.1
i-C_3H_7·	88.5 ± 1.0	106.2
$NH_2CH_2^+$	750.3 ± 1.0	763.9

known and fixed in the optimization. If the methyl radical heat of formation is also optimized, it only decreases by 0.1 kJ mol^{-1}, confirming the reliability of our approach.

Overall, Figure 8 suggests that the heats of formation of alkyl radicals, despite their associated error bars, are in fact better established than those of the primary alkylamines. The discrepancies between the initial and the optimized heats of formation are significant for methylamine, ethylamine, propylamine, butylamine, and the isopropyl radical. The errors in the TPEPICO results are all systematic and are related to the resolution and the accuracy of the RRKM model, because the statistics of each breakdown diagram are as reliable as reasonably possible. The *ab initio* errors are also nonstatistical. Therefore, the only statistical indication as to how accurate the revised heats of formation are lies with the difference between the (full) and the (nolink) fits, i.e., how well the TPEPICO and the *ab initio* results concur. On the basis of this criterion, we choose not to propose a new, more accurate heat of formation for butylamine due to the 1.3 kJ mol^{-1} inconsistency between the experimental and the *ab initio* fits, but it is indicated that its heat of formation is probably underestimated, and the associated error bar should be increased to at least 2.0 kJ mol^{-1}. The discrepancies are smaller for isobutylamine, but the accuracy of our result ($\Delta_f H^o_{298K}[i\text{-}C_4H_9NH_2(g)] = -97.8 \pm 1.0$ kJ mol^{-1}) is less than that of the previous measurement (-98.6 ± 0.5 kJ mol^{-1}).

The error minimization procedure has led us to propose new heats of formation for methylamine, ethylamine, propylamine, the propyl radical, and the *i*-propyl radical, which are based on the all-inclusive optimization with internal rotational corrections. Thus, $\Delta_f H^o_{298K}[CH_3NH_2(g)] = -21.8 \pm 1.5$ kJ mol^{-1}, $\Delta_f H^o_{298K}[C_2H_5NH_2(g)] = -50.1 \pm 1.5$ kJ mol^{-1}, $\Delta_f H^o_{298K}[C_3H_7NH_2(g)] = -70.8 \pm 1.5$ kJ mol^{-1}, $\Delta_f H^o_{298K}[C_3H_7^\bullet] = 101.3 \pm 1$ kJ mol^{-1}, and $\Delta_f H^o_{298K}[i\text{-}C_3H_7^\bullet] = 88.5 \pm 1$ kJ mol^{-1}. The ethylamine heat of formation is revised by -2.6 kJ mol^{-1}, a value practically equal to the reported -2.5 kJ mol^{-1} discrepancy based on group additivities in the Pedley compilation.[30] The changes and the associated uncertainties of the other alkylamine heats of formation are such that the previous literature values are within the uncertainty of the new values. Nearly all fits suggest that the methyl-, propyl-, butyl-, and isobutylamine heats of formation should be increased by at least 0.5 kJ mol^{-1}. Although it is rather improbable that this is a coincidence, more accurate heat of formation and vaporization heat measurements would be needed to confirm the systematic error in the previous literature values.

The only free radical heat of formation that has shifted substantially (by 1.5 kJ/ mol) from the Seakins[2] value of 90.0 $\pm$ 1.7 kJ mol^{-1} is that of i-C_3H_7. It is worthwhile to look at other literature values for this radical. The 298 K heat of formation is also listed in a 2003 NASA-JPL publication[45] as 86.6 $\pm$ 2 kJ mol^{-1}, and by Tsang[46] as 88 $\pm$ 2 kJ mol^{-1}. Lau and Ng[47] have used *ab initio* methods to predict the heat of formation of the isopropyl radical, and compared the results with those of Tschuikow-Roux and Chen.[48] It is interesting that our 298 and 0 K values (88.5 and 106.2 kJ mol^{-1}, respectively) agree best with the measured 298 K value of Tschuikow-Roux and Chen (87.9 kJ mol^{-1}) and the calculated 0 K value of Lau and Ng (105.2 kJ mol^{-1}). Lau and Ng convert the $\Delta_f H^o{}_{0K}{}^{calc} =$ 105.2 kJ mol^{-1} to $\Delta_f H^o{}_{298K}{}^{calc} = 90.0$ kJ mol^{-1} based on effective anharmonic CCSD(T)/6-311G(2df,p) vibrational frequencies, which seem to overestimate the overall thermal enthalpy.

Remarkably, the methylenimmonium ion heat of formation has remained constant in the optimization, with its value in the (full), (ROH), (RH), and (norot) fits being 750.3, 750.1, 750.7, and 750.4 kJ mol^{-1}, respectively. The (nolink) fit does not contain the TPEPICO dissociation energies, and is therefore insensitive to the value of the methylenimmonium ion heat of formation. Thus, the methylenimmonium ion heat of formation is accurate even though the methylamine heat of formation, on which its experimental value is based, is found to be in error. This can be ascribed to error cancellation. Based on the ion cycle and computational results, the errors in the ethyl and propyl radical heats of formation are below the respective error bars of 1.6$-$1.7 and 2.1 kJ mol^{-1} and can be decreased to $\pm$ 1 kJ mol^{-1}.

Conclusions

A number of primary alkylamines (RCH_2NH_2, R = H, CH_3, C_2H_5, C_3H_7, i-C_3H_7) have been studied with threshold photoelectron photoion coincidence spectroscopy. Two isodesmic reaction networks have also been constructed, one containing the primary alkylamines, i.e., the reactants of the photodissociation in the TPEPICO experiment, and the other consisting of the alkyl radicals, i.e., the products of the photodissociation. The link between the two isodesmic reaction networks is the methylenimmonium ion, which is the common product of the photodissociation of the amines. The 0 K dissociation energies for the amines RCH_2NH_2, R = CH_3, C_2H_5, C_3H_7, i-C_3H_7 have been measured to be 9.754 $\pm$ 0.008, 9.721 $\pm$ 0.008, 9.702 $\pm$ 0.012, and 9.668 $\pm$ 0.012 eV, respectively, and were used together with the previously determined dissociation energy for methylamine (10.228 $\pm$ 0.008 eV). The heats of formation of

the amines and the radicals have been optimized so that they are consistent with the measured TPEPICO dissociation energies and the computed isodesmic reaction heats.

The TPEPICO dissociation energies and the isodesmic reaction heats are 0 K properties, to which the thermal enthalpy is explicitly added. On the other hand, other experimental results usually yield thermochemical data in which the thermal enthalpy is inherently included. The description of the hindered internal rotation has been studied to account for its contribution to the 298 K dissociation energies and reaction heats. The internal rotation has little effect on the thermal enthalpies of the amines, but its contribution is about -1 kJ mol^{-1} for the alkyl radicals, in which a low barrier hindered internal rotor causes the harmonic approximation to introduce a considerable error. The agreement between the experimental heats of formation and our results is restored for the ethyl and propyl radicals when the hindered internal rotation is also considered.

Contrary to our expectations, the isodesmic networks with or without the TPEPICO dissociation energies suggested that the alkyl radical heats of formation are more accurately known than the alkylamine gas phase heats of formation. On the basis of the results, we suggest new heats of formation for methylamine, ethylamine, propylamine, and the isopropyl radical. The heats of formation of the methyl-, propyl-, butyl-, and isobutylamines appear to be systematically underestimated in the literature, but the accuracy of their new values does not allow for an incontrovertible conclusion in this regard. The optimized heats of formation of the ethyl and the propyl radical suggest that their error bars have been overestimated in previous measurements.

Acknowledgment. We are grateful to the U.S. Department of Energy and the international office of the National Science Foundation for financial support.

Supporting Information Available: A total of 45 reactions calculated at the two levels of theory; internal rotational curves calculated for all species (amines, alkanes, alcohols, and alkyl radicals); the calculated reaction enthalpies with the previous experimental amine and radical heats of formation from the literature and with the newly obtained ones. This material is available free of charge via the Internet at http://pubs.acs.org.

References and Notes

(1) Harvey, Z. A.; Traeger, J. C. *Eur. J. Mass Spectrom.* **2004**, *10*, 759−766.

(2) Seakins, P. W.; Pilling, M. J.; Niiranen, J. T.; Gutman, D.; Krasnoperov, L. N. *J. Phys. Chem.* **1992**, *96*, 9847−9855.

(3) Berkowitz, J.; Ellison, G. B.; Gutman, D. *J. Phys. Chem.* **1994**, *98*, 2744−2765.

(4) Dearden, D. V.; Beauchamp, J. L. *J. Phys. Chem.* **1985**, *89*, 5359−5365.

(5) Houle, F. A.; Beauchamp, J. L. *J. Am. Chem. Soc.* **1979**, *101*, 4067−4074.

(6) Schultz, J. C.; Houle, F. A.; Beauchamp, J. L. *J. Am. Chem. Soc.* **1984**, *106*, 3917−3927.

(7) Schultz, J. C.; Houle, F. A.; Beauchamp, J. L. *J. Am. Chem. Soc.* **1984**, *106*, 7336−7347.

(8) Baer, T.; Sztáray, B.; Kercher, J. P.; Lago, A. F.; Bodi, A.; Scull, C.; Palathinkal, D. *Phys. Chem. Chem. Phys.* **2005**, *7*, 1507−1513.

(9) Bodi, A.; Kercher, J. P.; Baer, T.; Sztáray, B. *J. Phys. Chem. B* **2005**, *109*, 8393−8399.

(10) Kercher, J. P.; Fogleman, E. A.; Koizumi, H.; Sztáray, B.; Baer, T. *J. Phys. Chem. A* **2005**, *109*, 939−946.

(11) Sztáray, B.; Baer, T. *Rev. Sci. Instrum.* **2003**, *74*, 3763−3768.

(12) Gengeliczki, Z.; Sztáray, B.; Baer, T.; Iceman, C.; Armentrout, P. B. *J. Am. Chem. Soc.* **2005**, *127*, 9393−9402.

(13) Lago, A. F.; Baer, T. *J. Phys. Chem. A* **2006**, *110*, 3036−3041.

(14) Lago, A. F.; Kercher, J. P.; Bodi, A.; Sztáray, B.; Miller, B. E.; Wurzelmann, D.; Baer, T. *J. Phys. Chem. A* **2005**, *109*, 1802−1809.

(15) Davalos, J. Z.; Koizumi, H.; Baer, T. *J. Phys. Chem. A* **2006**, *110*, 5032−5037.

(16) Kercher, J. P.; Sztáray, B.; Baer, T. *Int. J. Mass Spectrom.* **2006**, *249*, 403−411.

(17) Bodi, A.; Sztaray, B.; Baer, T. *Phys. Chem. Chem. Phys.* **2006**, *8*, 613−623.

(18) Frisch, M. J.; Trucks, G. W.; Schlegel, H. B.; Scuseria, G. E.; Robb, M. A.; Cheeseman, J. R.; Montgomery, J. A.; Vreven, T.; Kudin, K. N.; Burant, J. C.; Millam, J. M.; Iyengar, S. S.; Tomasi, J.; Barone, V.; Mennucci, B.; Cossi, M.; Scalmani, G.; Rega, N.; Petersson, G. A.; Nakatsuji, H.; Hada, M.; Ehara, M.; Toyota, K.; Fukuda, R.; Hasegawa, J.; Ishida, M.; Nakajima, T.; Honda, Y.; Kitao, O.; Nakai, H.; Klene, M.; Li, X.; Knox, J. E.; Hratchian, H. P.; Cross, J. B.; Adamo, C.; Jaramillo, J.; Gomperts, R.; Stratmann, F.; Yazyev, O.; Austin, A. J.; Cammi, R.; Pomelli, C.; Ochterski, J. W.; Ayala, P. Y.; Morokuma, K.; Voth, G. A.; Salvador, P.; Dannenberg, J. J.; Zakrzewski, V. G.; Dapprich, S.; Daniels, A. D.; Strain, M. C.; Farkas, Ö.; Malick, D. K.; Rabuck, A. D.; Raghavachari, K.; Foresman, J. B.; Ortiz, J. V.; Cui, Q.; Baboul, A. G.; Clifford, S.; Cioslowski, J.; Stefanov, B. B.; Liu, G.; Liashenko, A.; Piskorz, P.; Komáromi, I.; Martin, R. L.; Fox, D. J.; Keith, T.; Al-Laham, M. A.; Peng, C. Y.; Nanayakkara, A.; Challacombe, M.; Gill, P. M. W.; Johnson, B.; Chen, W.; Wong, M. W.; Gonzalez, C.; and Pople, J. A. Gaussian 03, Revision C.02. 2004. Pittsburgh PA, Gaussian, Inc.

(19) Chase, M. W. *NIST-JANAF Thermochemical Tables*; American Institute of Physics: New York, 1998.

(20) Wagman, D. D.; Evans, W. H. E.; Parker, V. B.; Schum, R. H.; Halow, I.; Mailey, S. M.; Churney, K. L.; Nuttall, R. L. *The NBS Tables of Chemical Thermodynamic Properties, J. Phys. Chem. Ref. Data Vol. 11 Suppl. 2*; NSRDS: U.S. Government Printing Office; Washington, 1982.

(21) Ochterski, J. W.; Petersson, G. A.; Montgomery, J. A. *J. Chem. Phys.* **1996**, *104*, 2598−2619.

(22) Brooks, A.; Lau, K.-C.; Ng, C. Y.; Baer, T. *Eur. J. Mass Spectrom.* **2004**, *10*, 819−828.

(23) Traeger, J. C.; McLoughlin, R. G. *J. Am. Chem. Soc.* **1981**, *103*, 3647−3652.

(24) Fogleman, E. A.; Koizumi, H.; Kercher, J. P.; Sztáray, B.; Baer, T. *J. Phys. Chem. A* **2004**, *108*, 5288−5294.

(25) Traeger, J. C.; McLoughlin, R. G.; Nicholson, A. J. C. *J. Am. Chem. Soc.* **1982**, *104*, 5318−5326.

(26) Lias, S. G. Ionization Energy Data: http://webbook.nist.gov/chemistry/ om/. 2006. Ref Type: Generic.

(27) Aue, D. H.; Web, H. M.; Bowers, M. T. *J. Am. Chem. Soc.* **1976**, *98*, 311−317.

(28) Watanabe, K.; Mottl, J. R. *J. Chem. Phys.* **1957**, *26*, 1773−1774.

(29) Aue, D. H.; Bowers, M. T. Stabilities of positive ions from equilibria in gas phase basicity measurements. In *Gas Phase Ion Chemistry*; Bowers, M. T., Ed.; Academic Press: New York, 1979; Vol. 2, pp 2−50.

(30) Pedley, J. B. *Thermochemical Data and Structures of Organic Compounds*; Thermodynamics Research Center: College Station, TX, 1994.

(31) Baboul, A. G.; Curtiss, L. A.; Redfern, P. C.; Raghavachari, K. *J. Chem. Phys.* **1999**, *110*, 7650−7657.

(32) Martin, J. M. L.; de Oliveira, G. *J. Chem. Phys.* **1999**, *111*, 1843−1856.

(33) Parthiban, S.; Martin, J. M. L. *J. Chem. Phys.* **2001**, *114*, 6014−6029.

(34) McClurg, R. B.; Flagan, R. C.; Goddard, W. A. I. *J. Chem. Phys.* **1997**, *106*, 6675−6680.

(35) Knyazev, V. *J. Chem. Phys* **1999**, *111*, 7161−7162.

(36) Press, W. H.; Teukolsky, S. A.; Vetterling, W. T.; Flannery, B. P. *Numerical Recipes in FORTRAN 77. The Art of Scientific Computing*; Cambridge University Press: Cambridge, 1992; pp 223−230.

(37) de Oliveira, G.; Martin, J. M. L.; Silwal, I. K. C.; Liebman, J. F. *J. Comput. Chem.* **2001**, *22*, 1297−1305.

(38) Raghavachari, K.; Stefanov, B. B.; Curtiss, L. A. *Mol. Phys.* **2005**, *91*, 555−560.

(39) Raghavachari, K.; Stefanov, B. B.; Curtiss, L. A. *J. Chem. Phys.* **1997**, *106*, 6764−6767.

(40) Ruscic, B.; Michael, J. V.; Redfern, P. C.; Curtiss, L. A. *J. Phys. Chem. A* **1998**, *102*, 10889−10899.

(41) Ruscic, B.; Pinzon, R. E.; Morton, M. L.; Laszevski, G.; Bittner, S. J.; Nijsure, S. G.; Amin, K. A.; Minkoff, M.; Wagner, A. F. *J. Phys. Chem. A* **2004**, *108*, 9979−9997.

(42) Lasdon, L. S. and Waren, A. D. *Generalized Reduced Gradient - 2 User's guide* (as implemented in the Excell program); School of Business Administration, University of Texas at Austin, 1986.

(43) Weitzel, K. M.; Malow, M.; Jarvis, G. K.; Baer, T.; Song, Y.; Ng, C. Y. *J. Chem. Phys.* **1999**, *111*, 8267−8270.

(44) Ruscic, B.; Boggs, J. E.; Burcat, A.; Csaszar, A. G.; Demaison, J.; Janoschek, R.; Martin, J. M. L.; Morton, M. L.; Rossi, M. J.; Stanton, J. F.; Szalay, P. G.; Westmoreland, P. R.; Zabel, F.; Berces, T. *J. Phys. Chem. Ref. Data* **2005**, *34*, 573−656.

(45) Sander, S. P.; Friedl, R. R.; Golden, D. M.; Kurylo, M. J.; Huie, R. E.; Orkin, V. L.; Moortgat, G. K.; Ravishankara, A. R.; Kolb, C. E.; Molina, M. J.; Finlayson-Pitts, B. J. *Chemical kinetics and photochemical; data for use in atmospheric studies*; JPL Publication 02-25, NASA/Jet Propulsion Laboratory: Pasadena, CA, 2003.

(46) Tsang, W. Heats of Formation of Organic Free Radicals by Kinetic Methods. In Energetics of Organic Free Radicals; Martinho Simões, J. A., Greenberg, A., Liebman, J. F., Eds.; Chapman & Hall: London, 1996; pp 22−58.

(47) Lau, K.-C.; Ng, C. Y. *J. Chem. Phys.* **2006**, *124*, 044323−1.-044323/9.

(48) Tschuikow-Roux, E.; Chen, Y. *J. Am. Chem. Soc.* **1989**, *111*, 9030−9031.

(49) Atkinson, R.; Baulch, D. L.; Cox, R. A.; Hampson, R. F.; Kerr, J. A.; Rossi, M. J.; Troe, J. *J. Phys. Chem. Ref. Data* **2000**, *29*, 167−266.